

On the identification of individual image types of a lensed system using higher-order modes

Justin Janquart^{1,2,*}, Eungwang Seo³, Otto A. Hannuksela^{1,2,3}, Tjonnje G. F. Li^{3,4,5}, and Chris Van Den Broeck^{1,2}

¹*Nikhef – National Institute for Subatomic Physics,
Science Park, 1098 XG Amsterdam, The Netherlands*

²*Institute for Gravitational and Subatomic Physics (GRASP), Department of Physics,
Utrecht University, Princetonplein 1, 3584 CC Utrecht, The Netherlands*

³*Department of Physics, The Chinese University of Hong Kong, Shatin, N.T., Hong Kong*

⁴*Institute for Theoretical Physics, KU Leuven, Celestijnenlaan 200D, B-3001 Leuven, Belgium and*

⁵*Department of Electrical Engineering (ESAT), KU Leuven,
Kasteelpark Arenberg 10, B-3001 Leuven, Belgium*

(Dated: October 14, 2021)

Similarly to light, gravitational waves can be gravitationally lensed as they propagate near massive astrophysical objects such as galaxies, stars, or black holes. In recent years, forecasts have suggested a reasonable chance of strong gravitational-wave lensing detections with the LIGO-Virgo-Kagra detector network at design sensitivity. As a consequence, methods to analyse lensed detections have seen rapid development. However, the impact of higher-order modes on the lensing analyses is still under investigation. In this work, we show that the presence of higher-order modes enables the identification of the individual images types for the observed gravitational-wave events when two lensed images are detected, which would lead to unambiguous identification of lensing. In addition, we show that we can analyse higher-order-mode content with greater accuracy with strongly lensed gravitational wave events.

I. INTRODUCTION

Similar to an electromagnetic wave, a gravitational wave (GW) can be deflected by a massive object along its path. This object is called a lens, and depending on its characteristics, it will have a different effect on the GW. For massive lenses, such as galaxies [1–4] or galaxy clusters [5–9], one can observe strong lensing, where several images of the GW are produced. These images will appear in the interferometers as repeated events with the same frequency evolution. However, the images have a different apparent luminosity distance (linked by a relative magnification), time of coalescence (linked by a time delay, going from seconds to months depending on the lens properties), and an overall phase shift (fully determined by the Morse factor) due to being focussed by the lens slightly differently [10, 11]. The Morse factor is a discrete parameter, taking three different values: 0, 0.5, and 1, corresponding to so-called type I, type II and type III images respectively [12].

Strong lensing is predicted to be observable with a reasonable rate ($\theta(1)$) in a network of 2G detectors at design sensitivity [2–4, 13, 14]. An example of a forecast is $1.7_{-0.6}^{+0.9} \text{ yr}^{-1}$ for a LIGO-Hanford, LIGO-Livingston, Virgo and KAGRA network, given in Ref. [14]) in the ground-based detectors such as Advanced Virgo [15], Advanced LIGO [16], and KAGRA [17–20] when they reach their design sensitivity. As a consequence, search techniques for strong lensing have been developed over

the last years [11, 21–24] and several searches for lensing signatures in the LIGO-Virgo data have been conducted [21, 22, 25, 26]. The science cases also now include studies spanning the domains of fundamental physics, astrophysics, and cosmology [27–41].

In parallel to lensing efforts, there have also been efforts to improve the quality of the waveform models used for the analysis of GW by adding higher-order modes (HOMs) [42–44] as their non-inclusion could lead to a loss in sensitivity for some systems and biases in the estimated parameters [45–47]. In addition to the improvement in the precision for the parameter inference [48–50], they could also improve various test of general relativity done with GWs [51–53].

The impact of such HOMs on lensing is explained in Ref. [54]. Usually, for a quasi-circular, non-precessing, binary black hole (BBH), the Morse phase is degenerate with the phase of coalescence so that the image type cannot be determined. However, this degeneracy can be lifted when HOMs are present, leading to a possible distinction of the Morse factor.

In Ref. [55], the authors studied the possibility to identify single type II images for current and future detectors. In Ref. [56], they show that not including the Morse factor in analysing a type II image with significant HOMs leads to biases in the inferred parameters. Moreover, they show that one can identify the lensed hypothesis and the image type when the HOM content is high enough. All these analyses focus on single images and require strong HOM contributions, which are not expected for the time being. A first demonstration of the possibility to identify image types based on two images is shown in Ref. [23] using a single exam-

* j.janquart@uu.nl

ple. Here, we go a step further by exploring a range of HOM contributions for the two images, investigating when the image identification is possible in general.

This work uses the joint parameter estimation framework Ref. [24] to analyse a pair of lensed images containing HOMs. We investigate whether detecting two images with HOMs will improve our ability to discriminate the image type. Furthermore, we investigate whether the observation of a lensed image pair would help study the HOMs present in the BBH system.

II. METHODOLOGY

Our objective is to identify the types of images present in an observed lensed image pair in this work. However, our ability to determine the image types depends on the HOM content of the event, as has been shown in Refs. [55] and [56]. Therefore, to explore different HOM contributions, we tune the HOM SNR by changing the mass ratio ($q = m_2/m_1$), the inclination (ι), and the luminosity distance (D_L) of the events. For the first image, the D_L is adapted so that the network SNR [57] for the event is always 12. For the mass ratio, the three values considered are 0.1, 0.3, 0.5, while for the inclinations we choose the values to be 20° , 45° , and 70° . When considering lensing, we also need to specify the image types, as well as the relative magnification (μ_{rel}) and time delay (Δt) between the two images. We consider three types of lensed systems in this work: type I–type II, type I–type I, and type II–type II, where a type I image has a Morse factor $n = 0$, and a type II image has $n = 0.5$. One could also have type III images, with $n = 1$. However, those are expected to be rare, as they would require lenses with very shallow central profiles [14] and are therefore not considered here. Throughout this work, the time delay between the two images is fixed at 11 hr while the relative magnification is such that the SNR of the second image has a specific value (we consider values of 12 or 25 for the second image as these represent a typical and a loud event one can expect based on current LVK observing runs [58]). The values for the other parameters are fixed to arbitrary values, kept identical for all the events (except if explicitly mentioned).

For each event, we inject the GW with the IMR-PHENOMXHM waveform [44] in a network of interferometers made of the two LIGO detectors and the Virgo detector at design sensitivity [15, 59] and do the recovery with IMRPHENOMXHM and IMRPHENOMD [60].

The priors used in these analyses and the general setup are the same as those presented in Ref. [24]. That is, the priors for the lensing parameters are uniform for the relative magnification and time delay, discrete uniform for the (difference in) Morse factor. Furthermore, we choose a uniform prior for the chirp mass, the mass

ratio, coalescence time, the cosine of the inclination angle, the polarisation angle, and the coalescence phase. The prior for the sky position is such that we have a uniform distribution for the location on a sphere, and the luminosity distance prior is uniform in the comoving distance.

III. RESULTS

Here, we first look at the possibility to identify the individual image types for an observed pair of lensed images. We also investigate how our ability to identify the image type evolves with the HOM content of the image pair, and contrast this with the scenario where only one image is detected. We focus on type I–type II systems for quantitative statements. The other systems are treated more qualitatively. We also look at the impact of analysing an event pair with HOM using a waveform that does not include them. Finally, we investigate whether our ability to discern the HOM content (and not only the image type) improves when we analyse two images jointly.

1. type I–type II systems

When HOMs are present with a high enough contribution, it is possible to distinguish individual type II images [55]. However, this requires very specific BBH systems that will not often be observed [56].

Here, we look at a system of type I and type II images and investigate our ability to recover the image types. Note that when performing the joint analysis, the difference in the Morse phase is always uniquely recovered (with $\Delta n = 0.5$ for the systems considered here). From this information already, one can directly infer that the first image is not a type III image. Thus, we choose $P(n_1 = n_1^{inj} | data) \geq 0.75$ as a criterion to determine that an event type is recovered correctly in the two-image case. This is the case, on average, once the HOM SNR is higher than $\rho_{HOM} = 0.5$. On the other hand, we cannot discard the type III image scenario directly for a single image. As a consequence, we choose $P(n_1 = n_1^{inj} | data) \geq 0.6$ as the criterion to determine that the event type is correctly identified in the case of single images. This threshold is crossed when $\rho_{HOM} \geq 1$. Consequently, the possibility to identify the image types of a lensed event pair can be done for a weaker HOM contribution than for a single type II image. A comparison between the evolution of $P(n_1 = n_1^{inj} | data)$ as a function of the HOM SNR can be seen in Fig. 1: The decision threshold is crossed for a lower ρ_{HOM} when two images are observed.

We note that the unequivocal recovery of the image types for an event pair would lead to smoking-gun

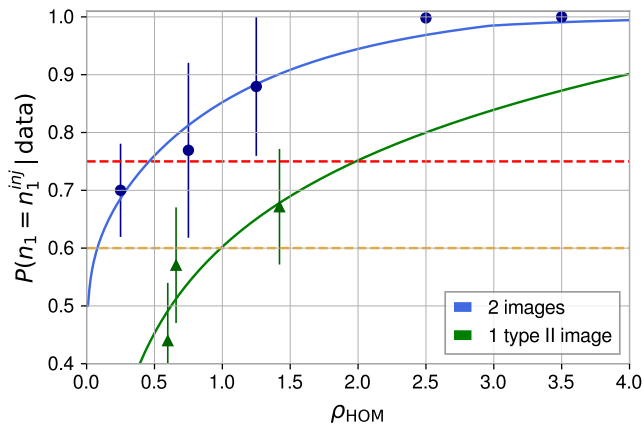


FIG. 1. Comparison between the posterior probability values for the injected Morse factor for a system made of type I and a type II image (in blue) and for a single type II image (in green) as a function of the (total) SNR of the HOMs. For the lensed system, the first image has a fixed SNR of 12, while the second image has an SNR of 12 or 25. We change the HOM content of the images by using different combinations of mass ratios and inclinations. For the single image systems, the SNR is fixed at 25 and we change the HOM content by varying the mass ratio and the inclination. The image type identification is made at lower total HOM content when two images are observed than when only one type II image is observed.

evidence for lensing as no other standard effect could reproduce similar results.

2. type I–type I and type II–type II systems

This work also considers other types of systems, namely, type I–type I systems and type II–type II systems. The ability to identify the image types for a given pair depends on the types of images present. When two type II images are detected, the image types can be identified at a lower total HOM SNR than for the observation of a single type II image.

On the other hand, we cannot identify the image types unequivocally for type I–type I systems, regardless of the HOM SNR. When the HOM SNR is high enough, it is possible to exclude the presence of a type II image, and we can say that the two images have the same type. Yet, we cannot determine the exact types of the images based uniquely on the GW data. The same is expected for a system made of type III images. However, type-III imaging is rare when considering a galaxy lens (which creates long lensing time delays). Therefore, the hypothesis of two type I images would be favoured. The likelihood of type-III imaging when considering galaxy-cluster lenses is less clear.

These observations show that we require at least one type II image to determine the image types based only on GW data.

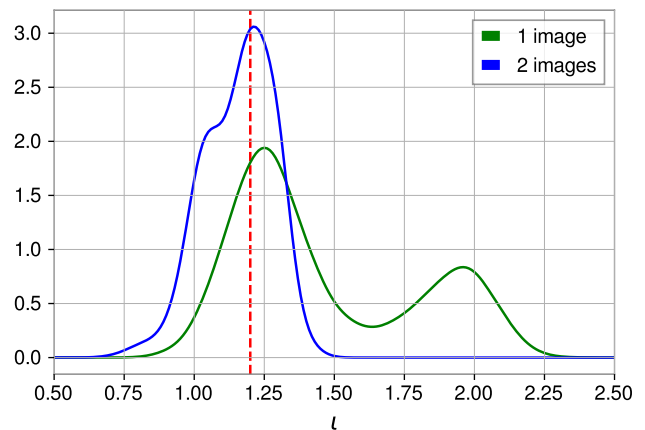


FIG. 2. The posterior distribution for the inclination for an unlensed event (in green) and a lensed image pair (in blue). The events have the same (total) network SNR (of 16.97), and the same $\rho_{\text{HOM}}/\rho_{\text{tot}}$ (of 0.14). The inclination is better constrained for the lensed images than for the unlensed event. Therefore, the HOM content can better be probed for a lensed image pair than for a single unlensed merger with the same HOM content.

3. Note about the recovery without HOMs for a system with HOMs

Without HOMs, the coalescence phase and the Morse phase are degenerate. Therefore, image type identification is not possible [54]. In addition, the non-inclusion of the HOM in the analysis of events containing significant HOMs can lead to biases in some parameters such as the polarisation angle, the phase, the distance [45, 46]. Since this bias will change depending on the antenna response of the detector (as the angle of view changes the HOM that can be probed), the two images making up the lensed system are biased differently. For a type I–type II system, when the HOM content is strong (e.g. $\rho_{\text{HOM}} = 3.5$), our framework is not able to detect lensing anymore when the analysis is made with IMRPHENOMD. This means that the frequency evolution between the two images is too different to match the two images.

4. Better measuring HOMs with lensing

We compare the results of one type I–type II image system with a single unlensed image, both having the same total SNR (with a value of 16.97 for $\sqrt{\sum_i \text{SNR}_i^2}$, where i runs over the images) and $\rho_{\text{HOM}}/\rho_{\text{tot}} = 0.14$. Therefore, we use the same BBH parameters for the different events, except for the polarisation angle and the (apparent) luminosity distance. So, the total HOM content is the same in both scenarios, enabling us to probe whether observing a lensed pair of events leads to a better ability to observe the HOM content.

The presence of HOMs allows us to constrain the

binary inclination better. In addition, this parameter can be used to characterise the constraints on the HOM content. The posterior distributions for the inclination in the two scenarios are represented in Fig.2. It shows that, for a given total HOM content, the observation of two images leads to a better measure of the HOMs content. This result, coupled with the possible image identification presented above, leads to the conclusion that the detection of two lensed images with a presence of HOM would allow us to study the HOM content with greater precision.

IV. CONCLUSION

In this work, we have focused on the impact lensing and HOMs can have on each other when observing a lensed image pair. We have shown that our ability to identify the strong lensing image type greatly improves when jointly analysing two images (as opposed to one). If we were to identify the presence of type-II images, it would count as smoking-gun evidence that the event is lensed. In addition, we have confirmed that the presence of a type II image is required to unequivocally identify the observed image types based uniquely on GW data. We have also shown that when the HOMs play an important role, their non-inclusion

in the lensing analysis can lead to the non-detection of a lensed pair. Finally, we have shown that strongly lensed gravitational-wave events allow us to study HOM content more accurately than (similar) non-lensed gravitational waves. Thus, the observation of a lensed event with HOMs would be beneficial to the study of HOMs.

ACKNOWLEDGEMENTS

The authors thank Juan Calderon Bustillo for his very useful input about HOMs for gravitational waves and for helping to decide the example events used in this work. We are also thankful to Apratim Ganguly, Aditya Vijaykumar, and Ajit Mehta for discussion on a related topic.

JJ, OAH, and CVDB are supported by the research program of the Netherlands Organisation for Scientific Research (NWO). TGFL and ES were partially supported by grants from the Research Grants Council of the Hong Kong (Project No. CUHK 14306218), The Croucher Foundation of Hong Kong and Research Committee of the Chinese University of Hong Kong. The authors are grateful for computational resources provided by the LIGO Laboratory and supported by the National Science Foundation Grants No. PHY-0757058 and No. PHY-0823459.

-
- [1] L. Dai, T. Venumadhav, and K. Sigurdson, *Phys. Rev. D* **95**, 044011 (2017), arXiv:1605.09398 [astro-ph.CO].
- [2] K. K. Y. Ng, K. W. K. Wong, T. Broadhurst, and T. G. F. Li, *Physical Review D* **97**, 023012 (2018), arXiv:1703.06319 [astro-ph.CO].
- [3] S.-S. Li, S. Mao, Y. Zhao, and Y. Lu, *Mon. Not. Roy. Astron. Soc.* **476**, 2220 (2018), arXiv:1802.05089 [astro-ph.CO].
- [4] M. Oguri, *Mon. Not. Roy. Astron. Soc.* **480**, 3842 (2018), arXiv:1807.02584 [astro-ph.CO].
- [5] G. P. Smith, M. Jauzac, J. Veitch, W. M. Farr, R. Massey, and J. Richard, *Mon. Not. Roy. Astron. Soc.* **475**, 3823 (2018), arXiv:1707.03412 [astro-ph.HE].
- [6] G. Smith *et al.*, *IAU Symp.* **338**, 98 (2017), arXiv:1803.07851 [astro-ph.CO].
- [7] G. P. Smith, A. Robertson, M. Bianconi, and M. Jauzac, arXiv e-prints, arXiv:1902.05140 (2019), arXiv:1902.05140 [astro-ph.HE].
- [8] A. Robertson, G. P. Smith, R. Massey, V. Eke, M. Jauzac, M. Bianconi, and D. Rychanowski, *mnras* **495**, 3727 (2020), arXiv:2002.01479 [astro-ph.CO].
- [9] D. Rychanowski, G. P. Smith, M. Bianconi, R. Massey, A. Robertson, and M. Jauzac, *Mon. Not. Roy. Astron. Soc.* **495**, 1666 (2020), arXiv:2005.02296 [astro-ph.GA].
- [10] Y. Wang, A. Stebbins, and E. L. Turner, *Phys. Rev. Lett.* **77**, 2875 (1996), arXiv:astro-ph/9605140.
- [11] K. Haris, A. K. Mehta, S. Kumar, T. Venumadhav, and P. Ajith, arXiv e-prints, arXiv:1807.07062 (2018), arXiv:1807.07062 [gr-qc].
- [12] L. Dai and T. Venumadhav, arXiv e-prints, arXiv:1702.04724 (2017), arXiv:1702.04724 [gr-qc].
- [13] F. Xu, J. M. Ezquiaga, and D. E. Holz, (2021), arXiv:2105.14390 [astro-ph.CO].
- [14] A. R. A. C. Wierda, E. Wempe, O. A. Hannuksela, L. V. E. Koopmans, and C. Van Den Broeck, (2021), arXiv:2106.06303 [astro-ph.HE].
- [15] F. Acernese *et al.* (VIRGO), *Class. Quant. Grav.* **32**, 024001 (2015), arXiv:1408.3978 [gr-qc].
- [16] J. Aasi *et al.* (LIGO Scientific), *Class. Quant. Grav.* **32**, 074001 (2015), arXiv:1411.4547 [gr-qc].
- [17] K. Somiya (KAGRA), *Class. Quant. Grav.* **29**, 124007 (2012), arXiv:1111.7185 [gr-qc].
- [18] Y. Aso, Y. Michimura, K. Somiya, M. Ando, O. Miyakawa, T. Sekiguchi, D. Tatsumi, and H. Yamamoto (KAGRA), *Phys. Rev. D* **88**, 043007 (2013), arXiv:1306.6747 [gr-qc].
- [19] T. Akutsu *et al.* (KAGRA), *Nature Astron.* **3**, 35 (2019), arXiv:1811.08079 [gr-qc].
- [20] T. Akutsu *et al.*, arXiv e-prints, arXiv:2005.05574 (2020), arXiv:2005.05574 [physics.ins-det].
- [21] L. Dai, B. Zackay, T. Venumadhav, J. Roulet, and M. Zaldarriaga, arXiv e-prints, arXiv:2007.12709 (2020), arXiv:2007.12709 [astro-ph.HE].
- [22] X. Liu, I. Magaña Hernandez, and J. Creighton, *Astrophys. J.* **908**, 97 (2021), arXiv:2009.06539 [astro-ph.HE].

- [23] R. K. L. Lo and I. Magana Hernandez, arXiv e-prints , arXiv:2104.09339 (2021), arXiv:2104.09339 [gr-qc].
- [24] J. Janquart, O. A. Hannuksela, K. Haris, and C. Van Den Broeck, arXiv e-prints , arXiv:2105.04536 (2021), arXiv:2105.04536 [gr-qc].
- [25] O. A. Hannuksela, K. Haris, K. K. Y. Ng, S. Kumar, A. K. Mehta, D. Keitel, T. G. F. Li, and P. Ajith, *Astrophys. J. Lett.* **874**, L2 (2019), arXiv:1901.02674 [gr-qc].
- [26] R. Abbott *et al.* (LIGO Scientific, Virgo), (2021), arXiv:2105.06384 [gr-qc].
- [27] M. Sereno, P. Jetzer, A. Sesana, and M. Volonteri, *Mon. Not. Roy. Astron. Soc.* **415**, 2773 (2011), arXiv:1104.1977 [astro-ph.CO].
- [28] T. Baker and M. Trodden, *Phys. Rev. D* **95**, 063512 (2017), arXiv:1612.02004 [astro-ph.CO].
- [29] X.-L. Fan, K. Liao, M. Biesiada, A. Piorowska-Kurpas, and Z.-H. Zhu, *Phys. Rev. Lett.* **118**, 091102 (2017), arXiv:1612.04095 [gr-qc].
- [30] K. Liao, X.-L. Fan, X.-H. Ding, M. Biesiada, and Z.-H. Zhu, *Nature Commun.* **8**, 1148 (2017), [Erratum: *Nature Commun.* **8**, 2136 (2017)], arXiv:1703.04151 [astro-ph.CO].
- [31] K.-H. Lai, O. A. Hannuksela, A. Herrera-Martín, J. M. Diego, T. Broadhurst, and T. G. F. Li, *Phys. Rev. D* **98**, 083005 (2018), arXiv:1801.07840 [gr-qc].
- [32] S. Cao, J. Qi, Z. Cao, M. Biesiada, J. Li, Y. Pan, and Z.-H. Zhu, *Sci. Rep.* **9**, 11608 (2019), arXiv:1910.10365 [astro-ph.CO].
- [33] Y. Li, X. Fan, and L. Gou, *Astrophys. J.* **873**, 37 (2019), arXiv:1901.10638 [astro-ph.CO].
- [34] S. Mukherjee, B. D. Wandelt, and J. Silk, *Phys. Rev. D* **101**, 103509 (2020), arXiv:1908.08950 [astro-ph.CO].
- [35] S. Mukherjee, B. D. Wandelt, and J. Silk, *Mon. Not. Roy. Astron. Soc.* **494**, 1956 (2020), arXiv:1908.08951 [astro-ph.CO].
- [36] S. Goyal, K. Haris, A. K. Mehta, and P. Ajith, *Phys. Rev. D* **103**, 024038 (2021), arXiv:2008.07060 [gr-qc].
- [37] J. M. Diego, *Phys. Rev. D* **101**, 123512 (2020), arXiv:1911.05736 [astro-ph.CO].
- [38] O. A. Hannuksela, T. E. Collett, M. Çalişkan, and T. G. Li, *Mon. Not. Roy. Astron. Soc.* **498**, 3395 (2020), arXiv:2004.13811 [astro-ph.HE].
- [39] M. Oguri and R. Takahashi, *Astrophys. J.* **901**, 58 (2020), arXiv:2007.01936 [astro-ph.CO].
- [40] P. Cremonese, J. M. Ezquiaga, and V. Salzano, (2021), arXiv:2104.07055 [astro-ph.CO].
- [41] A. Finke, S. Foffa, F. Iacovelli, M. Maggiore, and M. Mancarella, (2021), arXiv:2107.05046 [gr-qc].
- [42] A. Kumar Mehta, P. Tiwari, N. K. Johnson-McDaniel, C. K. Mishra, V. Varma, and P. Ajith, *Phys. Rev. D* **100**, 024032 (2019), arXiv:1902.02731 [gr-qc].
- [43] G. Pratten *et al.*, *Phys. Rev. D* **103**, 104056 (2021), arXiv:2004.06503 [gr-qc].
- [44] C. García-Quirós, M. Colleoni, S. Husa, H. Estellés, G. Pratten, A. Ramos-Buades, M. Mateu-Lucena, and R. Jaume, *Phys. Rev. D* **102**, 064002 (2020), arXiv:2001.10914 [gr-qc].
- [45] J. Calderón Bustillo, S. Husa, A. M. Sintes, and M. Pürrer, *Phys. Rev. D* **93**, 084019 (2016), arXiv:1511.02060 [gr-qc].
- [46] V. Varma and P. Ajith, *Phys. Rev. D* **96**, 124024 (2017), arXiv:1612.05608 [gr-qc].
- [47] B. P. Abbott *et al.* (LIGO Scientific, Virgo), *Class. Quant. Grav.* **34**, 104002 (2017), arXiv:1611.07531 [gr-qc].
- [48] K. G. Arun, B. R. Iyer, B. S. Sathyaprakash, S. Sinha, and C. Van Den Broeck, *Phys. Rev. D* **76**, 104016 (2007), [Erratum: *Phys.Rev.D* **76**, 129903 (2007)], arXiv:0707.3920 [astro-ph].
- [49] L. London, S. Khan, E. Fauchon-Jones, C. García, M. Hannam, S. Husa, X. Jiménez-Forsteza, C. Kalaghatgi, F. Ohme, and F. Pannarale, *Phys. Rev. Lett.* **120**, 161102 (2018), arXiv:1708.00404 [gr-qc].
- [50] P. Kumar, J. Blackman, S. E. Field, M. Scheel, C. R. Galley, M. Boyle, L. E. Kidder, H. P. Pfeiffer, B. Szilagyi, and S. A. Teukolsky, *Phys. Rev. D* **99**, 124005 (2019).
- [51] P. T. H. Pang, J. C. Bustillo, Y. Wang, and T. G. F. Li, *Phys. Rev. D* **98**, 024019 (2018).
- [52] P. D. Lasky, E. Thrane, Y. Levin, J. Blackman, and Y. Chen, *Phys. Rev. Lett.* **117**, 061102 (2016), arXiv:1605.01415 [astro-ph.HE].
- [53] C. Talbot, E. Thrane, P. D. Lasky, and F. Lin, *Phys. Rev. D* **98**, 064031 (2018), arXiv:1807.00990 [astro-ph.HE].
- [54] J. M. Ezquiaga, D. E. Holz, W. Hu, M. Lagos, and R. M. Wald, *Phys. Rev. D* **103**, 064047 (2021), arXiv:2008.12814 [gr-qc].
- [55] Y. Wang, R. K. L. Lo, A. K. Y. Li, and Y. Chen, *Phys. Rev. D* **103**, 104055 (2021).
- [56] A. Vijaykumar, A. Ganguly, and A. Mehta, in prep.
- [57] B. S. Sathyaprakash and B. F. Schutz, *Living Rev. Rel.* **12**, 2 (2009), arXiv:0903.0338 [gr-qc].
- [58] R. Abbott *et al.* (LIGO Scientific, VIRGO), (2021), arXiv:2108.01045 [gr-qc].
- [59] L. Barsotti, P. Fritschel, M. Evans, and S. Gras, “Advanced LIGO anticipated sensitivity curves,” <https://dcc.ligo.org/LIGO-T1800044/public> (2021).
- [60] S. Khan, S. Husa, M. Hannam, F. Ohme, M. Pürrer, X. J. Forsteza, and A. Bohé, *Phys. Rev. D* **93**, 044007 (2016).